

Differentiation of Holographic-moiré Patterns

Holographic multiplexing techniques are used to obtain full-field strain measurements by optically shearing holographic-moiré component and/or displacement patterns

by John A. Gilbert

ABSTRACT—Partial derivatives of displacement are optically determined by superimposing two shifted holographic reconstructions which correspond to single components of displacement. Two different methods are proposed, one of which involves shifting a holographic-moiré pattern on itself. A second method takes advantage of holographic multiplexing techniques to incorporate an initial pattern into the shifting process. The latter facilitates the formation of the moiré corresponding to strain information. This paper demonstrates that either method of obtaining derivatives is feasible by documenting an investigation of a disk subjected to diametral compression.

List of Symbols

d = displacement vector
 e_i = propagation vector
 \hat{e}_i = unit vector in the direction of propagation
 n_i = fringe-order number
 p = pitch
 x, y, z = coordinates of the reference system
 u, v, w = scalar components of the displacement
 z_c = coordinate of the center of rotation
 z_p = coordinate of the photographic plate
 D = diameter of the disk
 P = object point
 α = sensitivity angle
 β = angle of rotation of the photographic plate
 δ = fringe spacing
 ϵ_{ij} = components of the strain tensor
 θ_r = reference-beam angle
 Δ = increment
 λ = wavelength
 ϕ_β = phase change of the initial pattern

Introduction

A simple method which can be used to optically obtain partial derivatives of moiré patterns is to superimpose two identical patterns slightly shifted with respect to one another.^{1,2} Similar methods have been applied to differentiate geometrical patterns in spatial-filtering applications,³ speckle-interferometric investigations,⁴ and in conjunction with the shadow-moiré technique.⁵

The present investigation proposes two shifting methods which can be applied to holographic interferometry. Multiplexing techniques allow one to obtain full-field strain measurements by optically shearing holographic-moiré component and/or displacement patterns.

Analysis

The holographic-moiré technique uses a collimated dual-beam illumination to project the displacement vector of each model point along a common sensitivity vector over the full field. The method has been applied to flat surfaces,⁶ curved surfaces,⁷ and to points inside transparent solids.⁸ Image-plane methods have been used to suppress speckle noise and to record high-density fringe gradients of good quality.⁹

Figure 1 shows a point P on a diffusely reflecting surface illuminated with two beams corresponding to propagation vectors e_1 and e_2 and observed from a point corresponding to the propagation vector e_3 . Displacement-phase relations can be written for the case when the point is displaced between holographic recordings as,

$$n_1\lambda = -(\hat{e}_1 - \hat{e}_3) \cdot d + \phi_\beta \quad (1)$$

and

$$n_2\lambda = -\{\hat{e}_2 - \hat{e}_3\} \cdot d + \phi_\beta \quad (2)$$

where n_1 and n_2 are the fringe-order numbers corresponding to the holographic component patterns observed, d is the displacement vector, λ is the wavelength, and \hat{e}_i are unit vectors in the direction of propagation. The additional phase change ϕ_β is documented in Ref. 6 and represents an initial pattern of fringes caused by a rotation of the photographic plate between exposures.

Since both of the component patterns are observed along e_3 , they can be viewed simultaneously and the resulting superposition is characterized by a moiré pattern given by,

$$\lambda(n_1 - n_2) = \lambda n_m = (\hat{e}_2 - \hat{e}_1) \cdot d \quad (3)$$

where n_m is the moiré-fringe order number. Note that eq (3) is independent of the observation direction and the phase change ϕ_β .

Equations (1) and (2) can be referred to the axes system shown and are expressed in terms of the scalar displacement components (u, v, w) and the sensitivity angle, α , as

John A. Gilbert is Assistant Professor, Department of Mechanics, University of Wisconsin—Milwaukee, Milwaukee, WI 53201.

Original manuscript submitted: December 22, 1977. Final version received: March 27, 1978.

$$\lambda n_1 = u \sin \alpha + w(1 + \cos \alpha) + \phi_\beta \quad (4)$$

and

$$\lambda n_2 = -u \sin \alpha + w(1 + \cos \alpha) + \phi_\beta \quad (5)$$

Similarly, eq (3) becomes,

$$\lambda n_m = 2u \sin \alpha \quad (6)$$

That is, the moiré pattern represents a single component of displacement; namely, u .

The pattern corresponding to eq (6) can now be shifted through a Δx to give rise to a moiré pattern described by,

$$\frac{\Delta u}{\Delta x} \cong \frac{\partial u}{\partial x} = \frac{\lambda n_{mx}}{2 \Delta x \sin \alpha} \quad (7)$$

where n_{mx} is the resulting fringe-order number. The isoparagoc pattern observed in the shifting process corresponds to the difference in the orders of pairs of points that happen to coincide in the shifted arrangement.

The value of $\frac{\Delta u}{\Delta x}$ is the average value over the shifted interval and the precise value of the partial derivative at some point in the interval.

Shifting this same pattern through Δy , one obtains,

$$\frac{\Delta u}{\Delta y} \cong \frac{\partial u}{\partial y} = \frac{\lambda n_{my}}{2 \Delta y \sin \alpha} \quad (8)$$

where n_{my} is the resulting fringe-order number.

Similar arguments can be applied to a symmetrical dual-beam illumination in the yz plane to obtain $\frac{\partial v}{\partial x}$ and $\frac{\partial v}{\partial y}$.

No 'small-deformation' restriction has been introduced by the shifting process and the method is valid for large deformations. Hence, the four partial derivatives can be used to obtain the nonlinear normal and shear-strain components; however, for the small strains and small rotations determined with holography, the shifted patterns give the conventional strains directly. Lagrangian and Eulerian values are approximately equal, and the corresponding strain-tensor terms reduce to,

$$\epsilon_{xx} = \frac{\partial u}{\partial x} \quad (9)$$

$$\epsilon_{yy} = \frac{\partial v}{\partial y} \quad (10)$$

$$\epsilon_{xy} = \frac{1}{2} \left(\frac{\partial u}{\partial y} + \frac{\partial v}{\partial x} \right) \quad (11)$$

An inherent difficulty in this shifting method, however, arises from the fact that the patterns corresponding to eqs (7) and (8) are moiré of moiré patterns. In order to establish n_{mx} and n_{my} , the displacement pattern given by eq (6) must have a sufficient number of isothetic fringes which are properly oriented to give rise to a visible interference pattern when the fringes are shifted on themselves. In general, this is not the case.

The same problem was previously encountered in the formation of the displacement pattern. That is, the holographic component patterns alone did not have suitable fringe gradient, spacing and orientation to produce a visible moiré. This problem was solved by rotating the photographic plate between exposures. The additional phase change ϕ_β which has been included in eqs (4) and

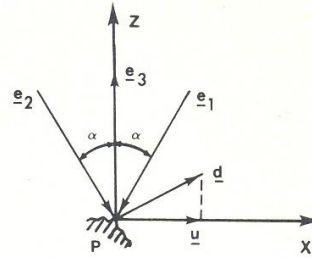


Fig. 1—Displacement analysis of a point P

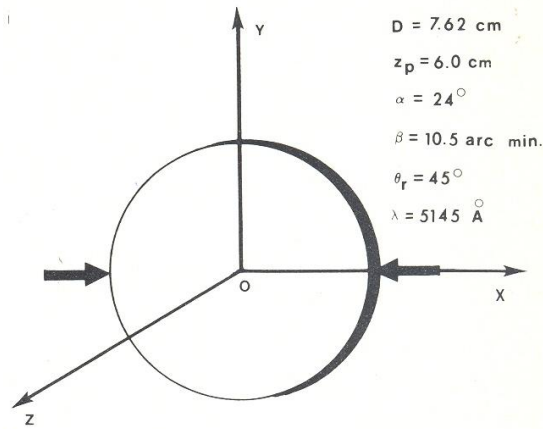


Fig. 2—Disk and coordinate system

(5), allowed the superposition of the component patterns to be realized.

The use of a mismatch to facilitate the forming of a moiré is an old concept that has been around for a long time.¹⁰ An alternate method which can be used to obtain derivatives is to take advantage of holographic multiplexing techniques to incorporate the initial pattern into the shifting process. To this end, consider shifting each of the component patterns corresponding to eqs (4) and (5), respectively, on themselves through a Δx . One obtains the following,

$$\frac{\lambda n_{1x}}{\Delta x} = \frac{\Delta u}{\Delta x} \sin \alpha + \frac{\Delta w}{\Delta x} (1 + \cos \alpha) + \frac{\Delta \phi_\beta}{\Delta x} \quad (12)$$

$$\frac{\lambda n_{2x}}{\Delta x} = -\frac{\Delta u}{\Delta x} \sin \alpha + \frac{\Delta w}{\Delta x} (1 + \cos \alpha) + \frac{\Delta \phi_\beta}{\Delta x} \quad (13)$$

where n_{1x} and n_{2x} are the resulting fringe-order numbers. The moiré patterns become visible with the aid of the initial pattern and can either be numerically subtracted or superimposed to form a moiré of a moiré. That is,

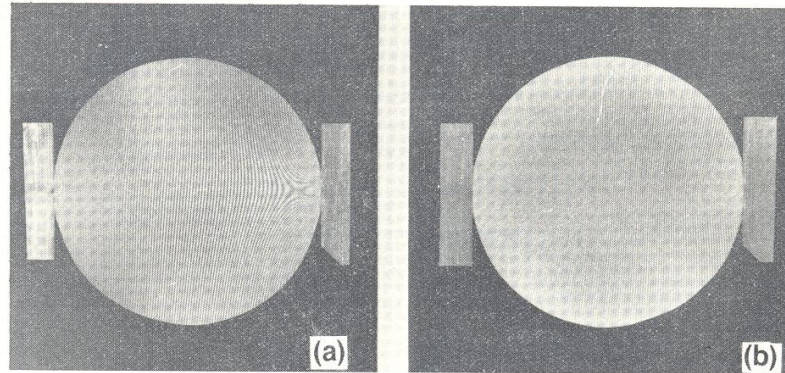
$$\frac{\lambda}{\Delta x} (n_{1x} - n_{2x}) = \frac{\lambda}{\Delta x} n_{mx} = 2 \frac{\Delta u}{\Delta x} \sin \alpha \quad (14)$$

and

$$\frac{\Delta u}{\Delta x} \cong \frac{\partial u}{\partial x} \equiv \epsilon_{xx} = \frac{\lambda n_{mx}}{2 \Delta x \sin \alpha} \quad (15)$$

(a) Illumination from the left
(b) Illumination from the right

Fig. 3—The component patterns



The result in eq (15) is analogous to that found in eq (7). Similar arguments can be developed to find $\frac{\partial u}{\partial y}$, $\frac{\partial v}{\partial x}$, and $\frac{\partial v}{\partial y}$. These values are related to the strain in eqs (9), (10) and (11).

The accuracy of both shifting methods is governed by the spacing and orientation of the displacement fringes, the amount of shift and the magnitude of the deformation. A small shift gives rise to more-precise fringe locations but affords less response than a larger shift for a given deformation. On the other hand, the larger the deformation, the smaller the shift needed to produce the same result.

This paper demonstrates that either method of obtaining derivatives is feasible by investigating a disk subjected to diametral compression.

Experimental

The disk and associated coordinates are shown in Fig. 2. Geometrical parameters and pertinent information used during this investigation are also documented on this figure. The experimental setup is based on Fig. 1. Two collimated beams, contained in the xz plane, illuminate the model. The photographic plate is supported in a kinematic device which has controlled displacement in the z direction, and is located on a stage which allows rotations to be made around an axis parallel to y .

The position of the center of rotation, z_c , is chosen in order to localize the initial pattern at the object surface by

satisfying the relation,

$$z_c = z_p \cos \theta_r \quad (16)$$

where z_p is the z coordinate of the photographic plate and θ_r is the angle subtended by the reference beam and the normal to the photographic plate; in this case, the latter is parallel to z . When the photographic plate is rotated through an angle β and no displacement is initiated to the model, the initial pattern has fringe spacing, δ , given by

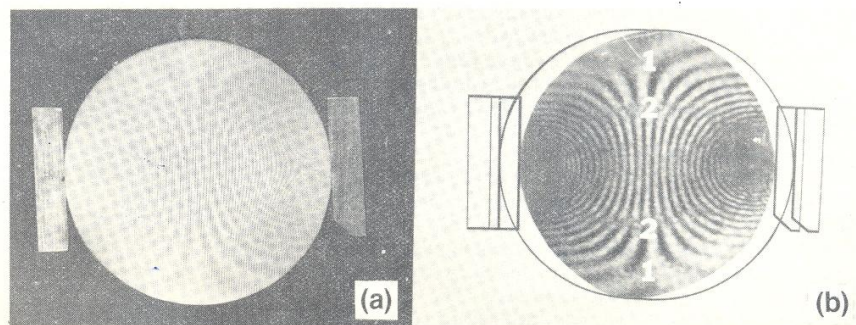
$$\delta = \frac{\lambda(z_p - z_c)}{\beta z_p \cos \theta_r} \quad (17)$$

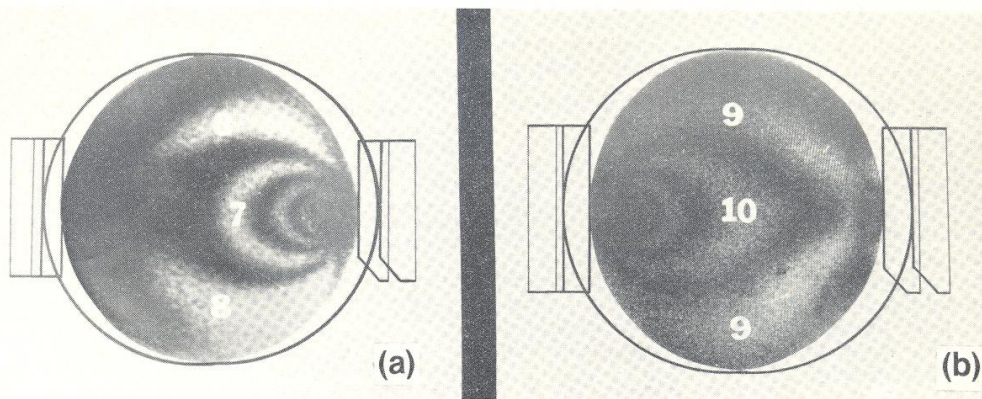
Equations (16) and (17) have been derived in Ref. 6 using a slightly different coordinate system.

In order to demonstrate both of the shifting methods proposed, each of the component patterns must be captured separately. To this end, a coarse grating of pitch p equal to 3.18 mm is modified so that the dark lines are slightly larger than the light ones. The grating is positioned in a kinematic device which allows translation perpendicular to the grid. This multiplexing unit is placed in the reference beam. One component pattern is recorded with the grating in its initial position while the second component pattern is recorded with the grating shifted through $p/2$. The information corresponding to each pattern is recorded in alternating strips which can be reconstructed separately with the grating in the appropriate position.

(a) Moiré-displacement pattern
(b) Shifted-displacement pattern

Fig. 4—Shifting the displacement pattern





(a) Illumination from the left
(b) Illumination from the right

Fig. 5—Filtered-shifted-component patterns

The original modification in the grating was initiated to eliminate any cross interference effects caused by diffraction at the edges of the grating and to prevent any overlap of the recording strips. Both images can be reconstructed simultaneously with the grating in an intermediate position. Furthermore, the grating can be positioned to favor one reconstruction over the other in the event that the two holographic recordings are of unequal intensity.

Note that this multiplexing method allows the component patterns to be recorded with the same spatial frequency. This is necessary when the initial pattern is incorporated into the component patterns. The localization and the fringe spacing, which depends upon θ , must be common to each of the component patterns for the holographic-moiré method to be valid. In addition, the grating should be positioned so that the recording strips are perpendicular to the rotation axis of the photographic plate to ensure that they are shifted parallel to themselves when the plate

is rotated between exposures. The latter avoids misalignment of the strips and a possible overlap of the two separate images during reconstruction.

The unloaded model state was first recorded with an illumination from the left with the reference grating in its initial position. The grating was shifted and the unloaded state was registered with an illumination from the right. The model was loaded and the photographic plate rotated. The deformed state was recorded with the reference grating in the shifted position, with an illumination from the right. The grating was then placed in its original position and the deformed state recorded with an illumination from the left.

The reconstruction of the component patterns is shown in Fig. 3. Figure 4(a) shows the moiré pattern, governed by eq (6), which is produced when these patterns are simultaneously reconstructed.

In order to demonstrate the first shifting method, the moiré displacement pattern was optically filtered and shifted on itself through a $\frac{\Delta x}{D}$ of 0.08, where D is the diameter of the disk. The shifted moiré pattern is shown in Fig. 4(b). The moiré of a moiré-fringe order numbers for points lying along the vertical center line were substituted into eq (8). The resulting strain is plotted in Fig. 6 along with theoretical values.

The second shifting method was verified when the component patterns were shifted on themselves through the same shift as that given to the displacement pattern in the method previously illustrated. Fringe-order numbers were determined by observing the moiré patterns develop in real time while two identical reconstructions of each component pattern were shifted on themselves. The unfiltered, shifted component patterns were optically filtered to improve fringe contrast and are shown in Figs. 5(a) and 5(b). The difference between the fringe-order numbers of the two moiré patterns determines n_{mx} in eq (15). The corresponding strain is plotted in Fig. 6 for points along the vertical center line of the disk.

A comparison of the results of both methods with the theory indicates a very close correlation; however, in general, errors will be larger than those observed in this experiment. As previously mentioned, the value of $\frac{\Delta u}{\Delta x}$

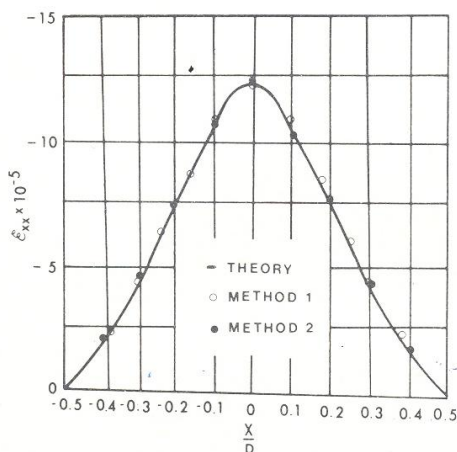


Fig. 6—A comparison of results: Method 1—shifted-displacement pattern; Method 2—shifted-component patterns

is the average value over the shifted interval and the precise value of the partial derivative at some point in the interval. In this case, the average and the precise values of $\frac{\Delta u}{\Delta x}$ coincide along the line of interest, resulting in no appreciable error.

In conclusion, full-field strain measurements have been obtained using two different shifting techniques. Shifting of the component patterns offers one distinct advantage over directly shifting the displacement pattern. That is, even though multiplexing and numerical subtraction are necessary in this method, plate rotation can be incorporated directly into each shifted pattern to facilitate the formation of the moiré corresponding to strain information. A study is underway to further improve these methods with image-plane holography.

Acknowledgment

This investigation was made possible through a grant from the Graduate School at the University of Wisconsin-Milwaukee and National Science Foundation Grant No. SER77-06858.

References

1. Parks, V.J. and Durelli, A.J., "Moiré Patterns of Partial Derivatives of Displacement Components," *J. Appl. Mech.*, **33**, Series E(4), 901-906 (1966).
2. Sciammarella, C.A. and Chang, T.Y., "Optical Differentiation of the Displacement Pattern Using Shearing Interferometry by Wavefront Reconstruction," *EXPERIMENTAL MECHANICS*, **11** (3), 97-104 (Mar. 1971).
3. Chiang, F.P., "Differentiation of Moiré Patterns by Optical Spatial Filtering," *J. Appl. Mech.*, **42**, Series E(1), 25-28 (1975).
4. Hung, Y.Y., Rowlands, R.E. and Daniel, I.M., "Speckle-Shearing Interferometric Technique: A Full-Field Strain Gage," *Appl. Optics*, **14** (3), 618-622 (1975).
5. Pirodda, L., "Optical Differentiation of Geometrical Patterns," *EXPERIMENTAL MECHANICS*, **17** (11), 427-432 (Nov. 1977).
6. Sciammarella, C.A. and Gilbert, J.A., "A Holographic-moiré Technique to Obtain Separate Patterns for Components of Displacement," *EXPERIMENTAL MECHANICS*, **16** (6), 215-220 (Jun. 1976).
7. Gilbert, J.A., Sciammarella, C.A. and Chawla, S.K., "Extension to Three Dimensions of a Holographic-moiré Technique to Separate Patterns Corresponding to Components of Displacement," *EXPERIMENTAL MECHANICS*, **18** (9), 321-327 (Sept. 1978).
8. Sciammarella, C.A. and Gilbert, J.A., "Holographic Interferometry Applied to the Measurement of the Displacements of the Interior Points of Transparent Bodies," *Appl. Optics*, **15** (9), 2176-2182 (1976).
9. Gilbert, J.A. and Exner, G.A., "Holographic Displacement Analysis Using Image-plane Techniques," *EXPERIMENTAL MECHANICS*, **18** (10), 382-388 (Oct. 1978).
10. Beranek, W.J., "Rapid Interpretation of Moiré Photographs," *EXPERIMENTAL MECHANICS*, **8** (6), 249-256 (Jun. 1968).